



Published in final edited form as:

*Clin Cancer Res.* 2017 July 01; 23(13): 3352–3364. doi:10.1158/1078-0432.CCR-16-2199.

## Expression of CD14, IL-10 and tolerogenic signature in dendritic cells inversely correlate with clinical and immunological response to TARP vaccination in prostate cancer patients

Luciano Castiello<sup>\*,1,2</sup>, Marianna Sabatino<sup>1</sup>, Jiaqiang Ren<sup>1</sup>, Masaki Terabe<sup>3</sup>, Hanh Khuu<sup>1</sup>, Lauren V Wood<sup>3</sup>, Jay A Berzofsky<sup>3</sup>, and David F Stronck<sup>1</sup>

<sup>1</sup>Cell Processing Section, Department of Transfusion Medicine, Clinical Center, National Institutes of Health, Bethesda, Maryland, USA

<sup>2</sup>Istituto Pasteur-Fondazione Cenci Bolognetti, Rome, Italy

<sup>3</sup>Vaccine Branch, Center for Cancer Research, National Cancer Institute, National Institutes of Health, Bethesda, Maryland, USA

### Abstract

**Purpose**—Despite the vast number of clinical trials conducted so far, Dendritic cell (DC)-based cancer vaccines have mostly shown unsatisfactory results. Factors and manufacturing procedures essential for these therapeutics to induce effective anti-tumor immune responses have yet to be fully characterized. We here aimed to identify DC markers correlating with clinical and immunological response in a prostate carcinoma vaccination regimen.

**Experimental Design**—We performed an extensive characterization of DCs used to vaccinate 18 prostate carcinoma patients enrolled in a pilot trial of TCR gamma alternate reading frame protein (TARP) peptide vaccination (NCT00908258). 114 peptide-pulsed DC preparations manufactured were analyzed by gene expression profiling, cell surface marker expression and cytokine release secretion and correlated with clinical and immunological responses.

**Results**—DCs showing lower expression of tolerogenic gene signature induced strong antigen-specific immune response and slowing in prostate-specific antigen (PSA) velocity, a surrogate for clinical response. These DCs were also characterized by lower surface expression of CD14, secretion of IL-10 and MCP-1; and greater secretion of MDC. When combined, these four factors were able to remarkably discriminate DCs that were sufficiently potent to induce strong immunological response.

**Conclusion**—DC factors essential for the activation of immune responses associated with TARP vaccination in prostate cancer patients were identified. This study highlights the importance of in-depth characterization of DC vaccines – and other cellular therapies, to understand the critical factors that hinder potency and potential efficacy in patients.

## Keywords

Dendritic cells; cancer vaccine; prostate carcinoma; cancer immunotherapy

---

## Introduction

Dendritic cells (DCs) are antigen presenting cells that are able to activate both innate and adaptive arms of the immune system(1). For this reason DC-based vaccines represent a promising immunotherapeutic approach in several clinical settings. In fact, since the discovery of monocyte differentiation into DCs(2), over 300 clinical trials have been conducted which have proven the feasibility and safety of DC vaccines(3). However, despite extensive preclinical and clinical studies, very few clinical trials have demonstrated the desired clinical efficacy. For the majority of trials, the overall response rates have been well below 20%(4). Many reasons have been hypothesized for such low response rates, among which the generation of DCs with suboptimal potency is considered the most relevant(4). It's not known yet how to generate the most potent DCs; furthermore, differences in clinical setting, study design, sources of antigens, and route of administration make it almost impossible to compare results from previously conducted trials in order to clearly delineate the shared determinants of *in vivo* efficacy of DC-based vaccines.

Compared to drug therapy, cell therapies are more challenging because of their considerable lot-to-lot and patient-specific variability that in most cases has yet to be sufficiently quantified and characterized (5). In fact, while each cell therapy lot has to be tested for identity, consistency and potency among other tests, feasibility issues dictate these tests to be focused on a handful of factors and, therefore, they cannot assure an exhaustive characterization of each lot. An accurate characterization of DCs should ideally assay all the factors affecting their *in vivo* biological functions: antigen processing and presentation, expression of co-stimulatory signals, absence or reduced expression of co-inhibitory signals, lymph node migration, and secretion of activating cytokines and chemokines. These are all essential features of potent DCs and should be thoroughly tested. Since it is impossible to routinely evaluate each product for every cell function using cellular assays, the identification of reliable biomarkers of identity, consistency and potency of cell therapies is highly encouraged by regulatory agencies beginning in the earliest phases of clinical development of the cellular product (6).

Many factors are known to play a key role in DC-induced activation of the immune system. Secretion of interleukin-12 (IL-12) is considered the most important driving factor for Th1 inflammatory T cell activation(7). Surface expression of CCR7 is necessary for DC migration into lymph nodes and expression of co-stimulatory molecules (i.e., CD80 and CD86) is essential for the activation of naive T cells (8). On the other hand, several detrimental factors have also been identified. Secretion of IL-10 is considered a hallmark of tolerogenic activities exerted by DCs(8,9). Similarly, the maintenance of immature/monocytic factors (e.g., CD14) are also known to be characteristic of tolerogenic DCs(10,11). Even though these and many other molecular factors have been characterized thoroughly for their role in DC function and many of them have been used to discriminate

among DCs produced using different differentiation/maturation procedures, it has rarely been determined how these factors are differentially expressed among DCs manufactured using the same differentiation/maturation procedure and whether such difference has a functional relevance.

Recently, our group has shown that even when highly standardized procedures are used to generate monocyte-derived DCs, manufacturing, intra-donor and inter-donor related factors may affect DC phenotype(12). In particular, we observed that while most of the well-known and usually tested DC markers (e.g., CD80, CD86, CD83, HLA-DR) did not show any differences in the expression among DCs generated at different times from different donors, the expression of several genes and the levels of several key secreted cytokines and chemokines showed significant variability among DC products. However, whether such lot-to-lot variability affects the identity, potency and/or efficacy of DC-based vaccines used in human clinical trials has yet to be determined.

NCI-09-C-0139 (NCT00908258) is a randomized, prospective, pilot study of vaccination with a mixture of wild type (TARP27-35) and epitope-enhanced (TARP29-37-9V) T cell receptor gamma chain alternative reading frame protein (TARP) peptides in HLA-A\*0201 patients with stage D0 prostate cancer (status post definitive treatment of primary tumor, with prostatectomy or radiotherapy, no evidence of visceral or bone metastasis with persistently elevated or rising PSA levels i.e. biochemical progression) and at increased risk for disease progression based on PSA doubling time (PSADT)(13). In stage D0 prostate cancer, the rate of change of PSA as slope or doubling time has been documented to be a valid predictor of clinical outcome (14). TARP is a tumor-associated antigen expressed in over 90% of prostate and 50% of breast carcinomas (15). The study compared two vaccination regimens: in one, TARP peptides were admixed with Montanide ISA 51 VG plus Sargramostim to generate a peptide emulsion administered by deep subcutaneous injection; in the other, TARP peptide-pulsed autologous dendritic cells (DCs) were administered intradermally. TARP DC vaccines were manufactured and administered every three weeks at weeks 3, 6, 9, 12, and 15 as part of the primary vaccination series, with a conditional sixth booster at week 36 dependent on documented immunologic and/or clinical responses at week 24. The original 48 week study design was amended and extended to subsequently allow seventh and/or eighth booster doses of vaccine at weeks 48 and 96 after initial immunologic and clinical activity of TARP vaccination was documented.

In the current study we analyzed 114 peptide-pulsed DC preparations manufactured to vaccinate 18 patients randomized to the autologous TARP peptide-pulsed DC arm in order to understand which factors are affected by lot-to-lot variability in clinical GMP manufactured DCs and whether such variability has an impact on DC identity, potency and efficacy. By analyzing DC surface marker expression, gene expression profiles, protein secretion profiles and culture data, we observed the existence of a tolerogenic DC signature that was negatively correlated with the development of clinical and immunological response.

## Materials and Methods

### Mature Dendritic Cell Manufacturing Process

DCs were manufactured according to a standard operating procedure established in the Cell Processing Section (CPS), Department of Transfusion Medicine (DTM), Clinical Center (CC), NIH, Bethesda, Maryland, USA. Briefly, peripheral blood mononuclear cell (PBMC) concentrates were collected by apheresis using a Cobe Spectra Apheresis System (Terumo BCT, Lakewood, CO, USA) from 18 patients enrolled in clinical trial NCI-09-C-0139 (NCT00908258). All patients signed an informed consent approved by the NCI Institutional Review Board. Monocytes were enriched directly from the leukapheresis products by elutriation using the Elutra Cell Separation System (Terumo BCT) according to the manufacturer's recommendations. Monocytes were cryopreserved in aliquots of  $300 \times 10^6$  cells. DCs were manufactured from single monocyte aliquots after assessing post-thaw viability and purity; in all cases both were greater than 80%. At the time of culture initiation, thawed monocytes were re-suspended in RPMI-1640 media, containing 10% autologous heat inactivated (HI) plasma, 10 mcg/ml gentamicin, GM-CSF (LeukineSargramostin, 2000 IU/ml, Genzyme, Cambridge, MA, USA) and IL-4 (USP grade recombinant human IL-4, 2000 IU/ml, CellGenix, GmbH, Freiburg, Germany) at a final concentration of  $1.5 \times 10^6$ /mL in tissue culture flasks (Corning Incorporated Life Sciences, Lowell, MA, USA) and incubated at 37° in 5% CO<sub>2</sub>. On day 2, fresh cytokines were added to the culture at the same concentrations together with keyhole limpet hemocyanin (KLH, 10 mcg/mL, Stellar Biotechnology Port Hueneme, CA, USA). On day 3 a maturation cocktail containing lipopolysaccharide (LPS) (30 ng/ml, CTEP, NIH Frederick, MD) and interferon gamma (IFN- $\gamma$ ) (Actimmune Interferon gamma-1b, 1000 IU/ml, Intermune, Brisbane, CA, USA) was added. 24 hours later DCs were harvested. After two washes DC were re-suspended in infusion media made of Plasma-Lyte A and 10% autologous heat-inactivated plasma. DCs were then pulsed in separate aliquots with wild type (WT) 27-35 and epitope-enhanced (EE) 29-37-9V TARP peptides (NeoMPS, Inc., San Diego, CA) at 37° in 5% CO<sub>2</sub>. After pulsing, DCs pulsed with the two peptides were combined and tested for recovery, viability, purity, sterility, mycoplasma absence, endotoxin concentration and expression of surface markers by flow cytometry (see below). Release criteria for each lot were defined based on CD83 expression by flow cytometry and trypan blue viability set as 70% and 60% respectively. If the cells met all the release criteria, then 20 million viable DCs were used for vaccination and were administered intradermally to patients. The remaining cells were centrifuged, and the supernatant was used for cytokine profile analysis (see below) and excess DCs were used for RNA extraction.

### Flow Cytometric analysis

Analysis of expression of surface markers was performed using fluorescent labeled antibodies (Abs) and flow cytometry. The purity of the elutriated monocytes was assessed by flow cytometry using CD33-PE, CD15-FITC, CD3/CD19/CD56-APC and CD45-APC-Cy7 (Becton Dickinson, Mountain View, CA, USA) and isotype controls (Becton Dickinson). DC were analyzed after pulsing on Day 4. The analysis included the standard "DC panel" adopted in our institution as lot release for mature DC products and other investigational markers. The panel consisted of CD86-FITC, CD83-PE, CD14-APC, HLA-DR-FITC,

CD123-PE, CD11c-APC, CD80-FITC, CD54-APC, CCR7-APC, and CD38-FITC (Becton Dickinson). Flow cytometry acquisition and analysis were performed with a FACScanto flow cytometer (Becton, Dickinson and Company, Franklin Lakes, NJ USA) according to CPS standard operating procedures. Spectral overlaps were electronically compensated using single color controls. Quality controls were run before each session according to internal quality control policy.

### Gene Expression Profiling

Total RNA was extracted from the unused fraction of DCs using an miRNeasy kit (Qiagen, Valencia, CA, USA). Universal Human Reference RNA (Stratagene, Santa Clara, CA, USA) was used as reference. Test samples and reference RNA were amplified and labeled using an Agilent kit according to the manufacturer's instructions and hybridized on Agilent Chip (Whole Human genome, 4×44k, Agilent Technologies, Santa Clara, CA, USA). The arrays were scanned using an Agilent Microarray Scanner and images analyzed using Agilent Feature Extraction Software 9.5.1.1. The resulting data were uploaded onto mAdb Gateway (<http://madb.nci.nih.gov>), the Agilent-normalized processed signals retrieved and analyzed with BRB Array Tools (<http://linus.nci.nih.gov/BRB-ArrayTools.html>). The processed data set was subjected to filtration based on signal intensity, quality and presence across the data set. A total of 35,753 genes passing these criteria were selected and log 2 base ratios were used for further analysis.

### Protein Analysis Platform

Supernatants of DC-conditioned infusion media were collected, stored at -80°C and analyzed all together at the end of the collection. The levels of 11 soluble factors were further assessed on a customized antibody-based platform (Aushon, Boston, MA, USA) consisting of a multiplex array with 11 different monoclonal antibodies spotted per well in standard 96-well plates. A sandwich enzyme-linked immunosorbent assay technique was used to generate signals via chemiluminescent substrate. Light corresponding to each spot in the array was captured by imaging entire plates with a commercially available cooled charge-coupled device (CCD) camera. Data were reduced using image analysis software (Aushon Proteome Arrays, Boston, MA, USA) that calculates exact values (pg/mL) based on standard curves. Prior to further analysis, protein concentrations were normalized according to the number of DCs.

**Evaluation of Immunological Response**—Patient evaluation of immunological response was performed as described in Wood et al (13). For the in vitro stimulation, frozen PBMC were thawed, re-suspended, and plated into wells of 24-well tissue culture plates (Corning, 3524) in media containing a 1:1 ratio of RPMI (Gibco, 21870-084) and Click's Medium (Sigma, C5572), 10% human AB serum (Gemini, 100-512), 1% Pen/Strep-L-glutamine (Gibco, 10378-016), 1% sodium pyruvate (Gibco, 11360-070), 35mM HEPES (Gibco, 15630-080) and 50 uM 2-mercaptoethanol (Sigma, M7522). On day 0, PBMC were stimulated with a mixture of TARP WT 27-35, TARP WT 29-37, and TARP EE 29-37 peptides at 10 ug/mL in the presence of 1000 u/mL recombinant human IL-7 (Peprotech, 200-07). On day 3, recombinant human IL-2 (Teceleukin; Roche, 23-6019) was added (20 u/

mL). On day 5 and 6, half of the culture supernatant was replaced with fresh CTL media and the cells were harvested on day 7 and 8.

All ELISPOT assays were performed in the Laboratory of Cell-Mediated Immunity at Leidos Biomedical Research, Inc. (formerly SAIC-Frederick, Inc.) which is certified by Clinical Laboratory Improvements Amendments (CLIA). Day7/8 IVS PBMC as the effectors and peptide-pulsed autologous day 0 PBMC as the antigen presenting cells (APC) were cocultured at a 1:1ratio ( $2.5 \times 10^4$  or  $10^5$  cells). The APC were pulsed with 10  $\mu$ g/mL TARP or control peptides 2 h at 37°C before being plated with the effectors.

The day before assay setup, 96-well polyvinylidene fluoride (PVDF) membrane, HTS opaque plates (Millipore, MSIPS4W10) were coated overnight with a 1:100 dilution of anti-human IFN $\gamma$  capture antibody (1 mg/mL, Mabtech 3420-3-1000) in DPBS. Antibody-coated plates were washed in DPBS and blocked with 5% human AB ELISPOT medium. The effectors and APC were plated and incubated for 18–20 h. Then, the plates were washed six times with 0.05% Tween 20 in DPBS. Plates were incubated for 2-h with a 1:2000 dilution of the biotinylated secondary antibody, anti-human IFN $\gamma$  (1 mg/mL Mabtech, 3420-6-1000) in DPBS/1% bovine serum albumin/0.05% Tween and then washed four times in DPBS. A 1:3000 dilution of streptavidin alkaline phosphatase (Mabtech, 3310-10) in DPBS/1% bovine serum albumin, was added to each well for 1 h followed by four washes in DPBS. Finally, the BCIP/NPT substrate, 100  $\mu$ L/well, (KPL, 50-81-07) was added for 7–10 min, resulting in the development of spots. Three washes in distilled water were performed to stop reaction. Spots were visualized and counted on overnight-dried plates using the ImmunoSpot Imaging Analyzer system (Cellular Technology Ltd.) and ImmunoSpot software v5.1. ELISPOT results were expressed as the “number of spots per  $10^6$  responder cells” after subtracting background spots obtained in wells of effectors with non-pulsed PBMC.

## Data Analysis

Receiver operating characteristic (ROC) curves were generated using the R package “pROC” (16). ROC curve represents an easy visualization tool because it illustrates the performance of the variable under study by plotting specificity vs sensitivity of the test for each possible cut-off; and the area under the curve (AUC) summarizes the overall ROC curve and can be considered as a summary statistic of its ability to classify cases correctly. A perfect test would have an AUC of 100%; a worthless test would have an AUC of 50%. According to an arbitrary guideline AUC values may be classified as follows: 90%–100%, excellent; 80%–90%, good; 70%–80%, fair; 60%–70%, poor; 50%–60%, fail (23). The area under the curve (AUC) was used as a measure of the performance of a classifier and confidence intervals were computed with Delong's method. Clinical responses as assessed by changes in slope log PSA (mathematically equivalent to an inverse calculated PSADT) at weeks 24 and 48 or strong immunological responses (defined as a TARP-specific interferon-gamma ELISPOT count > 500) were used to classify DCs. Clinical Response at week 24 was used for patient #203 that went off study during the trial.

Unsupervised hierarchical clustering and Principal Component Analysis (PCA) of the whole dataset were run with Partek Genomic Suite (Partek, St. Louis, MO, U.S.A.). Davies-



Bouldin Index was calculated with Partek to identify the number of clusters between 2 and 20 that better separates samples in subgroups. Class comparisons to identify genes differentially expressed among DCs were performed with BRB ArrayTools with a p-value threshold of 0.001. In order to control false discoveries, the False Discovery Rate (FDR) was calculated for each analysis as the ratio of the expected number of false discoveries divided by the number of discoveries as described by Sori (17).

Weighted Gene Co-expression Network Analysis (WGCNA) was performed using the R package “WGCNA” (18). The analysis was applied only on the most variable quartile (9112 genes) as suggested by package instructions. To apply more stringent criteria in module definition we applied a modification to standard protocol. The data set was split in two and WGCNA was then performed in both data sets. Only genes assigned to the same network in both analyses were considered as forming a module and used in subsequent analysis. Gene Ontology was performed using the Database for Annotation, Visualization and Integrated Discovery (DAVID, <http://david.abcc.ncifcrf.gov/>)(19) and Network analysis was performed using QIAGEN's Ingenuity Pathway Analysis (IPA®, QIAGEN Redwood City, CA, USA, [www.qiagen.com/ingenuity](http://www.qiagen.com/ingenuity)). The clustering of genes belonging to module 2 was performed with Cluster (20) and results were visualized with Java Treeview(21). For the meta-analysis, all publicly available tolerogenic DC data sets with clear sample information were selected from GEO and EMBL-EBI database. P-values were calculated with Fisher's exact test.

The data discussed in this publication have been deposited in NCBI's Gene Expression Omnibus (22) and are accessible through GEO Series accession number GSE85698 (<https://www.ncbi.nlm.nih.gov/geo/query/acc.cgi?acc=GSE85698>).”

CD14/IL10/MCP1/MDC index was calculated as follows: each DC preparation was ranked according to % of CD14+ cells and concentrations of IL-10, MCP-1 and MDC measured in supernatants in decreasing order (i.e., rank 1 to the highest expressing DC preparations). Then, taking into account that MDC levels negatively correlated with module 2, whereas CD14, IL-10 and MCP-1 levels positively correlated with module 2, the index was calculated as: MDC rank – (CD14 rank + IL-10 rank + MCP-1 rank). In this way, high index scoring DC preparations showed low expression of MDC and high expression of CD14, IL-10 and MCP-1.

## Results

### Clinical study and DC phenotype

Each DC vaccine was manufactured starting from one aliquot of autologous cryopreserved monocytes cultured for 3 days with GM-CSF and IL-4. On day 2, KLH was added to the culture as a control antigen. On day 3 cells were matured for additional 24 hours with LPS and IFN- $\gamma$  and then pulsed for 2 hours with WT and EE TARP peptides.

13 out of 16 evaluable patients were considered to have achieved a clinical response (decrease in slope log PSA) at week 48 (two additional patients completed the treatments but their week 48 clinical responses were not included as a result of the data analysis cut-off date for the dataset) (Wood et al., 2016 in press in OncoImmunology). The development of

TARP-specific immune response (assessed by IFN- $\gamma$ ELISPOT) was observed in 10 out of 18 evaluable patients (Interferon-gamma ELISPOT was performed on patient samples taken at baseline and weeks 12, 18 and 24 after vaccination). Immune activation against control antigen KLH was observed in the majority of patients (15 out of 16 subjects in whom KLH reactivity was assessed). Clinical (change in slope log PSA) and immunological responses were assessed both qualitatively (i.e., in terms of Responder or Non responder) and quantitatively (Table 1). Interestingly, slope log PSA responses were observed almost independently of TARP-specific T cell responses; however, a strong immunological response (defined as a median ELISPOT reading greater than 500) was observed only in patients with a notable decrease in slope log PSA ( $<0.045$ ; i.e., equivalent to a PSADT that at least doubles upon vaccination and therefore considered to indicate a stronger clinical response).

Notably, while patient baseline parameters were correlated (e.g., Gleason score and pre-vaccination PSA doubling time were correlated), clinical response was observed independently of pre-vaccination Gleason score ( $r^2 = 0.0438$ ), baseline PSA doubling time ( $r^2 = 0.0435$ ), or baseline PSA levels ( $r^2 = 0.0121$ ) (Supplemental Figure 1). As expected, clinical response assessed by the decrease in slope log PSA correlated with changes in PSA doubling time ( $r^2 = 0.6827$ ,  $p = 0.0012$ ), and PSA decline ( $r^2 = 0.4188$ ,  $p = 0.0067$ ).

Phenotypically all lots of DC products were positive for CD80, CD83, CD86, CD123, CD11c, CD38, CD54, HLA-DR (all  $> 95\%$ ) by flow cytometry (Figure 1A). The markers showing significant degrees of variability among DC products were CD14 (ranging from 14% to 90% CD14+) and CCR7 (ranging from 5% to 90%). This variability was dependent on both manufacturing and inter-patient factors, but only for CD14 the inter-patient variability was substantially greater than manufacturing variability (lot-to-lot for the same patient) (Figure 1B). Interestingly, when we analyzed DC preparations for differential expression among those from patients that achieved a decreasing slope log PSA clinical response (RespDC) versus those from patients that did not (NonRespDC), we observed a trend with RespDC expressing higher levels of CCR7 and lower levels of CD14 compared to NonRespDC (not statistically significant). To analyze how CCR7 or CD14 levels were able to discriminate RespDC vs NonRespDC we used receiver operating characteristic (ROC) analysis. The underlying assumption of ROC analysis is that a variable under study (e.g., % of CCR7+ DCs) is used to discriminate between two mutually exclusive states (i.e., RespDC vs NonRespDC). When qualitative clinical responses were evaluated by ROC curves both factors led to an Area Under the Curve (AUC) of 76.3% based on percent of CD14+ cells and of 69.6% based on percent of CCR7+ cells (Figure 1c).

In addition to phenotypic expression of surface markers we also analyzed cell culture data and noticed a great variability in final product viability and DC yield (i.e., the percentage of initial cells that were recovered at the end of DC manufacture), respectively ranging between 37% and 91% and between 6% and 48%. For these factors the sources of variability were also traced back to both manufacturing and inter-patient differences (Figure 1b). A non-random distribution was also observed for these factors between RespDC and NonRespDC, but with a much lower relevance (AUC based on DC viability was 60.8% and the AUC based on DC yield was 61%). All together these data indicate that lot-to-lot variability can



be observed in clinical DC products and that inter-patient variability might be responsible for phenotypic differences among RespDC and NonRespDC.

### DC transcriptomes clustered according to patient

Next, we analyzed gene expression profiles of 99 DC vaccine products derived from the 18 patients who received at least 5 vaccines using microarray technology. Unsupervised hierarchical clustering analysis grouped the DC products according to patient (Figure 2a), confirming the prominent role of inter-patient variability in affecting DC lot-to-lot variability shown in our previous report(12). In addition, the node analysis of the unsupervised hierarchical clustering did not show the existence of separated subclusters but rather indicated that the DC products were spread on continuum levels of variability as indicated by the fact that except for a few outlier samples, the vast majority of DC preparations showed similar inter-patient distances. Similar observations were obtained using principal component analysis (PCA) of the whole dataset and through Davies-Bouldin Index testing on partitioning the dataset into defined numbers of groups (not shown). Altogether these analyses suggested that clinical DC products show inter-patient differences that cannot be easily grouped into well-defined phenotypes. In particular, in both clustering and PCA analysis RespDC were not separated from NonRespDC, pointing to the fact that inter-patient variability exceeds any difference between RespDC and NonRespDC. Similar conclusions could be traced by standard class comparison analysis (see Supplemental Results) strongly suggesting that in order to delineate differences between RespDC and NonRespDC more complex models must be implemented in order to analyze inter-patient variability in an unbiased manner.

### Weighted Gene Coexpression Analysis revealed the presence of 8 modules in DCs

To characterize the inter-patient variability without any a priori assumption, we applied to our dataset the weighted gene coexpression analysis (WGCNA) in order to identify modules of genes that are coexpressed (i.e., whose expression changes similarly among different samples) and therefore should be strongly representative of inter-patient variability(18). WGCNA revealed the existence of 8 modules that were differentially expressed among the DC preparations in our dataset (Figure 2b). Modules were labeled numerically in decreasing order (i.e., Module 1 being the one made of the highest number of genes). Details about modules and the genes of which they are made are in Supplemental file 1. To dissect the characteristics of the eight modules and define whether the modules reflect manufacture-related variability or inter-patient variability, we calculated the manufacturing and inter-patient standard deviations for each module. As shown in Figure 2c while module 1 and 8 clearly showed a low level of inter-patient variability, the other modules showed a much higher degree of inter-patient variability indicating that differences in the expression levels of these modules exist among patient DCs (Figure 2c and d). Interestingly, modules 2, 3 and 7 showed low manufacturing related variability, suggesting that levels of expression of these modules are mainly affected by manufacturing-unrelated factors (Figure 2c). On the other hand, modules 4 and 6 were characterized by manufacturing-related variability levels comparable to inter-patient variability, indicating that genes belonging to these modules were more susceptible to manufacture-related variability.

### Low expression of Module 2 genes correlated with clinical and strong immunological responses

We then analyzed modules for their differential expression among RespDC and NonRespDC. Notably, only module 2 showed a statistically significant correlation with clinical response ( $R = 0.5278$ ,  $p\text{-value} = 0.035$ , Figure 3a), therefore suggesting that expression level of genes belonging to module 2 may play a role in clinical response. In particular, when we analyzed the expression of module 2 among different patient DC products, we observed that while up-regulation of module 2 led to mixed clinical responses, down-regulation of module 2 was strongly associated with clinical and immunological responses (Chi-square  $p\text{-value} = 0.008829$ , Figure 3b). Next, we evaluated module 2 expression for its predictive value for clinical response and through a ROC curve we obtained an AUC of 85.5% (Figure 3c). However, when tested as a predictor of strong immunological response, module 2 led to an almost perfect prediction with an AUC of 97.9%. All together these data indicate that lower expression of module 2 was correlated with more potent DC vaccines that resulted in strong immunological and clinical responses, even though clinical responses were observed even in patients that received DCs expressing high levels of module 2.

### Module 2 was a tolerogenic DC module

To characterize module 2 genes we performed a gene ontology (GO) analysis and among the most over-represented “biological process” GO families we observed: inflammatory response, immune response, chemotaxis, and endocytosis (Figure 3d). In particular, as shown by a network analysis (Figure 3e), the dominant module 2 factors were CD14, IL-10, thrombospondin, estrogen receptor 1, Insulin-like growth factor-binding protein 4, and hepatocyte growth factor (HGF). Most of these genes are known factors driving immune tolerance and specifically the first two are widely described as the major markers of tolerogenic DCs(10,24–27). To better understand whether module 2 represents a module of tolerogenic DCs, we performed a meta-analysis of all the publicly available tolerogenic DC gene expression studies and looked at how genes belonging to module 2 behaved in these other datasets of tolerogenic DC. In total, we found 8 gene expression datasets describing *in vitro* generated tolerogenic DC that could be used for the analysis. In these studies, tolerogenic DC were generated according to different protocols using IL-10 alone or in combination with other cytokines, mesenchymal stromal cells, T regulatory cells, or adhesion protein disruption. In 5 of the 8 analyzed datasets, we observed a statistically significance overlap of Module 2 overexpression in tolerogenic DCs (Table 2), strengthening the link between the expression of Module 2 genes and tolerogenic DCs.

### Low IL-10 concentrations correlated with strong immunological response

Next, we analyzed media supernatants obtained from the last 6 h of DC culture (see methods) in order to characterize the cytokine/chemokine secretion profiles of DC immediately before they were injected. We tested 93 supernatants (90 of which corresponding to the same DC we tested by gene expression) by ELISA for the presence of 11 proteins: IFN-gamma, IL-10, IL-12p70, IL-6, IP10 (CXCL10), MCP1 (CCL2), MIG (CXCL9), TNF-alpha, I-TAC (CXCL11), MDC (CCL22), and TGF-beta1. Interestingly, we

observed high levels of both manufacturing and inter-patient related variability for most of the tested proteins, with coefficients of variation ranging between 0.27 and 0.67 for manufacturing-related variability and between 0.33 and 1.34 for inter-patient related variability (Figure 4a). When tested for their predictive value of clinical response none of the proteins showed an AUC greater than 80% indicating that single cytokine concentrations in supernatants may not be good predictors of DC efficacy. However, when we tested protein concentrations for their predictive value of strong immunological response (similarly to what was observed with module 2 genes) we observed an impressive predictive value for IL-10 with an AUC of 95.8% (Figure 4b). In particular and as expected, minimal levels of IL-10 were detected in the supernatants of those DC that led to a strong immunological response compared to the ones that did not. A similar result was obtained when we tested the IL-12/IL-10 ratio. In this case, we observed an AUC of 94.3%, with the highest IL-12/IL-10 ratios leading to strong immunological responses (Supplemental figure 2).

### **Module 2 expression correlated with CD14, IL-10, MDC and MCP-1 secretion**

Given that it is not possible to routinely test DC by gene expression profiling, we analyzed how the expression of module 2 genes correlated with the other analyzed factors that can be tested more easily. As expected, we observed a statistically significant correlation between module 2 expression levels and percentages of CD14<sup>+</sup> DC assessed by flow cytometry ( $r = 0.71$ ,  $p\text{-value} < 0.0001$ ) and IL-10 secretion levels ( $r = 0.604$ ,  $p\text{-value} < 0.001$ ), confirming at a proteomic level, the observations made on gene expression profiles. Also, module 2 expression correlated positively with secreted concentrations of MCP-1 (CCL2) ( $r = 0.537$ ,  $p\text{-value} < 0.0001$ ) and negatively with level of MDC (CCL22) ( $r = -0.534$ ,  $p\text{-value} < 0.0001$ ). Given that none of these proteins was able to replace Module 2 for its predictive value as single factor, we evaluated whether by combining all four proteins we were able to obtain a better correlation with module 2. As shown in Figure 4c and better in Supplemental Figure 3, the combination of all 4 proteins correlated better with Module 2 expression. We, therefore, calculated for each DC product that we analyzed by gene expression, CD14 expression by flow and supernatant analysis by ELISA ( $n = 89$ ) a CD14/IL10/MCP1/MDC index (made by adding up DC ranks of the expression level of the 4 proteins, see methods for details) and observed that it strongly correlated with module 2 expression ( $R = 0.867$ ,  $p\text{-value} < 0.0001$ , Figure 4d). Next we tested its predictive value for both clinical and strong immunological responses and we obtained AUC of 88.7% and 97.2%, respectively (Figure 4e). Altogether, these data suggest that the analysis of CD14 expression by flow cytometry combined with IL-10, MCP-1 and MDC cytokine concentrations was able to discriminate between RespDC and NonRespDC.

## **Discussion**

DC-based cell therapies represent a promising approach to activate immune responses against tumors even though the vast majority of clinical trials have failed to show efficacy for such approach. Several reasons for such disappointing results have been identified: suboptimal generation and delivery of DCs, inappropriate selection of immunogenic tumor associated antigens, systemic inactivation of the immune system in advanced tumors and the ability of the established tumor microenvironment to inhibit T cell function. These factors

have all been widely described and analyzed as possible justification of poor clinical trial result outcomes(3,28–31). It has also been recently recognized that response evaluation of immunotherapies, especially cell-based therapies, should be based on different criteria compared to standard chemotherapy drugs and treatments, implying that the previous reports should be careful reevaluated(6).

In this study, we focused our analysis on the DC products administered to stage D0 prostate cancer patients, which allowed eliminating issues related to systemic tumor burden and a local immune-tolerizing microenvironment, and observed a strong correlation between DC phenotype and slope log PSA responses (a well-established surrogate for clinical outcomes in the stage D0 population) and immunological responses. In particular, we identified a gene signature made up of several well-known tolerogenic DC factors such as CD14 and IL-10 that was able to discriminate RespDc from NonRespDC. The differential expression of CD14 and IL-10 was confirmed at the proteomic level and observed that MCP-1 and MDC protein levels correlated (directly or inversely, respectively) with the expression level of the tolerogenic gene expression signature. Even though IL-10 secretion levels were able to predict strong immunological responses, it was only by combining CD14, IL-10, MCP-1 and MDC measures that it was possible to obtain an index able to replace the tolerogenic gene expression signature in its ability to discriminate both clinical and strong immunological responses.

Lot-to-lot variability is a critical issue for DC-based immunotherapies. Our data revealed a correlation between the phenotype of DCs used as vaccines and the induction of clinical and immunological responses. Even though functional analyses are needed to support a causative role of the identified phenotype, our observations further strengthen the need for extensive characterization of cellular products used in preclinical and early phase clinical trials in order to identify manufacturing and inter-patient related issues that may hamper identity, consistency and potency of final DC products. In a previous report, we described a framework for preclinical analysis of cell therapies for the identification of factors affecting consistency of cell products (12), but only by using accepted surrogates for clinical outcomes such as slope log PSA used in this study was it possible to correctly determine which factors play a role in product efficacy. The consistency of DC-based products is critical considering that many reports have highlighted how DC generated from patient monocytes show phenotypic differences compared to those manufactured from healthy donor monocytes (32–35). Therefore, lot-to-lot variability should be carefully characterized for each cell product in the early phases of product development to determine which factors should be analyzed routinely to control and manage product consistency.

The generation of potent DC capable of inducing a strong anti-tumor immune response is highly sought after, but a consensus concerning optimal DC generation protocols is still lacking. The changes in slope log PSA and TARP-specific immunogenicity following therapeutic vaccination observed in the current study were encouraging and highly statistically significant (13). Clinical responses were observed in 15 of 18 evaluable patients at 24 weeks and 13 out of 16 evaluable patients at 48 weeks, whereas immunological responses were detected in 10 out of 16 evaluable patients. However and more interestingly, our results suggest that even among DC products manufactured following identical standard

operating procedures it is possible to identify more potent DCs. The detrimental role of tolerogenic signals on DC function, such as expression of CD14 and secretion of IL-10, has been widely discussed in literature (8,10,27,36), but the direct involvement of these signals in clinical DC products has not yet been described. DC generated with our protocol and expressing low levels of tolerogenic genes, as determined by scoring low on our CD14/IL-10/MCP-1/MDC index, strongly correlated with the induction of strong immunological and clinical responses. How to more consistently manufacture DC with such a potent phenotype is under investigation in our laboratory, but the possibility of predicting which patients are more likely to benefit from vaccination is already an appealing scenario that will be tested further in forthcoming clinical trials at our institution.

DC culture conditions strongly affect DC phenotype: differentiation and maturation signals, their concentrations and the duration of stimulation strongly shape DC activity (3,8,36). In this study we focused in inter-patient and lot-to-lot DC phenotypic differences and identified gene and protein markers correlating with patient response. In particular, a lower expression of tolerogenic features was observed in patient that showed clinical and immunological response. Many factors may be the cause of the expression of tolerogenic genes and proteins in some DC vaccines: it has shown that individual genetic polymorphisms alter DC response to LPS(37,38), also patient serum levels of IL-10 or other cytokines can alter DC phenotype and activity(39,40). Therefore, it might be that for those patients whose DC show higher tolerogenic phenotype changes in manufacturing process could result in more potent DC vaccines, such as the use of different maturation signals (e.g., other TLR agonists) or replacement of autologous serum conditioned media with serum free ones(41).

Response to DC-based vaccine depends on several factors. In the current study, by analyzing DC administered to patients with relatively low tumor burdens i.e., micrometastatic disease since the only evidence of disease is PSA biochemical progression, we were able to more directly link DC phenotype with clinical and immune responses. However, it is reasonable to expect that in more complex clinical settings, additional factors related to DC phenotype as well as unrelated factors (e.g., overall patient immune system status following multiple chemotherapies, tumor phenotype and tumor burden) should also be considered. Therefore, complex data modeling should be developed in order to be able to extract precious information on DC phenotype and identify factors that correlate with clinical and immunologic outcomes. In our study, despite the clear induction of both clinical (81%) and immunological response (62.5%), there was no association between the two outcomes. This may depend on multiple factors. First, as pointed out by previous studies(42,43), clinical response may be the result of a minimal number of TARP specific T cells (and therefore undetectable by ELISPOT) that with their cytotoxic activity led to the activation of non-TARP specific T cells that are responsible of the clinical response. Moreover, DC may have exerted an antitumor effect by activating NK cells(44), B cells(45) or by a bystander activation of T cells (46). On the other side, it has to be considered that factors in the tumor microenvironment, such as programmed death-ligand 1 (PD-L1), cytotoxic T-lymphocyte-associated protein 4 (CTLA-4), myeloid-derived suppressor cells (MDSCs), tumor-associated macrophages, and T regulatory cells, are known to affect T cell response against tumor(47–49).

In this study, when we used standard statistical tools for the analysis of gene expression data (i.e., t-test based class comparison), we were not able to observe statistical differences among RespDC and NonRespDC. It was only when using a novel unsupervised method for the selection of gene modules which were co-expressed across the dataset (i.e., WGCNA) that we were able to uncover and identify the tolerogenic gene signature. In fact, some of RespDC did express similar levels of the tolerogenic signature of NonRespDC. What is the mechanism behind the ability of these DCs to induce clinical responses in the absence of a conventional immunological response will be tested in future clinical trials, but considering the multiplicity of effects DCs can exert(50), it is possible that these DCs worked by activating immune cells other than T cells (51) or that T cell responses in PBMC did not reflect localized tissue T cell responses that were more potent but could not be assessed. However, further investigations are needed to explore such hypotheses, including studies that involve expanded patient immunomonitoring and/or systems immunology.

To our knowledge this is the first study to perform an in-depth characterization of therapeutic DC vaccine products by combining flow cytometry phenotyping with gene expression profiling and cytokine/chemokine secretion profiling. With this approach we were able to observe a specific DC phenotype that correlated with the post vaccination clinical and immunological responses observed in this study. Although these data must be validated in a larger cohort of patients, they highlight the importance of extensive characterization of clinical and preclinical DC – as well as other cellular therapies, for the understanding of critical factors that may hinder their identity, consistency, potency and most important functional efficacy in patients. Once validated, these discoveries might allow the pre-treatment identification of patients that will more likely benefit from DC vaccine therapy and/or drive the development of manufacturing protocols that consistently lead to more potent DC.

## Supplementary Material

Refer to Web version on PubMed Central for supplementary material.

## Acknowledgments

This research was supported in part by the Intramural Research Program of the NIH, Department of Transfusion Medicine, Clinical Center and Vaccine Branch, Center for Cancer Research, National Cancer Institute.

## References

1. Ueno H, Schmitt N, Klechevsky E, Pedroza-Gonzalez A, Matsui T, Zurawski G, et al. Harnessing human dendritic cell subsets for medicine. *Immunol Rev.* 2010; 234:199–212. [PubMed: 20193020]
2. Sallusto F, Lanzavecchia A. Efficient presentation of soluble antigen by cultured human dendritic cells is maintained by granulocyte/macrophage colony-stimulating factor plus interleukin 4 and downregulated by tumor necrosis factor alpha. *J Exp Med.* 1994; 179:1109–18. [PubMed: 8145033]
3. Castiello L, Sabatino M, Jin P, Clayberger C, Marincola FM, Krensky AM, et al. Monocyte-derived DC maturation strategies and related pathways: a transcriptional view. *Cancer Immunol Immunother.* 2011; 60:457–66. [PubMed: 21258790]
4. Anguille S, Smits EL, Lion E, van Tendeloo VF, Berneman ZN. Clinical use of dendritic cells for cancer therapy. *Lancet Oncol.* 2014; 15:e257–67. [PubMed: 24872109]



5. Stroncek DF, Jin P, Ren J, Feng J, Castiello L, Civini S, et al. Quality assessment of cellular therapies: the emerging role of molecular assays. *Korean J Hematol.* 2010; 45:14–22. [PubMed: 21120158]
6. Vatsan, RS., Bross, PF., Liu, K., Theoret, M., De Claro, AR., Lu, J., et al. *J Immunother Cancer.* Vol. 1. BioMed Central Ltd; 2013. Regulation of immunotherapeutic products for cancer and FDA's role in product development and clinical evaluation; p. 5
7. Carreno, BM., Becker-Hapak, M., Huang, A., Chan, M., Alyasiry, A., Lie, WR., et al. *J Clin Invest.* Vol. 123. American Society for Clinical Investigation; 2013. IL-12p70–producing patient DC vaccine elicits Tc1-polarized immunity; p. 3383-94.
8. Kalinski P, Urban J, Narang R, Berk E, Wieckowski E, Muthuswamy R. Dendritic cell-based therapeutic cancer vaccines: what we have and what we need. *Future Oncol.* 2009; 5:379–90. [PubMed: 19374544]
9. Vieira PL, de Jong EC, Wierenga Ea, Kapsenberg ML, Kalinski P. Development of Th1-inducing capacity in myeloid dendritic cells requires environmental instruction. *J Immunol.* 2000; 164:4507–12. [PubMed: 10779751]
10. Torres-Aguilar H, Aguilar-Ruiz SR, González-Pérez G, Munguía R, Bajaña S, Meraz-Ríos Ma, et al. Tolerogenic dendritic cells generated with different immunosuppressive cytokines induce antigen-specific anergy and regulatory properties in memory CD4+ T cells. *J Immunol.* 2010; 184:1765–75. [PubMed: 20083662]
11. Chitta S, Santambrogio L, Stern LJ. GMCSF in the absence of other cytokines sustains human dendritic cell precursors with T cell regulatory activity and capacity to differentiate into functional dendritic cells. *Immunol Lett.* 2008; 116:41–54. [PubMed: 18166231]
12. Castiello L, Sabatino M, Zhao Y, Tumaini B, Ren J, Ping J, et al. Quality controls in cellular immunotherapies: rapid assessment of clinical grade dendritic cells by gene expression profiling. *Mol Ther.* 2013; 21:476–84. [PubMed: 23147403]
13. Wood LV, Fojo A, Roberson BD, Hughes MSB, Dahut W, Gulley JL, et al. TARP vaccination is associated with slowing in PSA velocity and decreasing tumor growth rates in patients with Stage D0 prostate cancer. *Oncoimmunology.* 2016; 5:e1197459. [PubMed: 27622067]
14. Vickers AJ, Brewster SF. PSA Velocity and Doubling Time in Diagnosis and Prognosis of Prostate Cancer. *Br J Med Surg Urol.* 2012; 5:162–8. NIH Public Access. [PubMed: 22712027]
15. Epel M, Carmi I, Soueid-Baumgarten S, Oh SK, Bera T, Pastan I, et al. Targeting TARP, a novel breast and prostate tumor-associated antigen, with T cell receptor-like human recombinant antibodies. *Eur J Immunol.* 2008; 38:1706–20. [PubMed: 18446790]
16. Robin X, Turck N, Hainard A, Tiberti N, Lisacek F, Sanchez JC, et al. pROC: an open-source package for R and S+ to analyze and compare ROC curves. *BMC Bioinformatics.* 2011; 12:77. [PubMed: 21414208]
17. Sori , B. *J Am Stat Assoc.* Vol. 84. Taylor & Francis; 1989. Statistical “Discoveries” and Effect-Size Estimation; p. 608-10.
18. Langfelder P, Horvath S. WGCNA: an R package for weighted correlation network analysis. *BMC Bioinformatics.* 2008; 9:559. [PubMed: 19114008]
19. Huang DW, Sherman BT, Lempicki R a. Systematic and integrative analysis of large gene lists using DAVID bioinformatics resources. *Nat Protoc.* 2009; 4:44–57. [PubMed: 19131956]
20. Eisen MB, Spellman PT, Brown PO, Botstein D. Cluster analysis and display of genome-wide expression patterns. *Proc Natl Acad Sci.* 1998; 95:14863–8. [PubMed: 9843981]
21. Saldanha AJ. Java Treeview--extensible visualization of microarray data. *Bioinformatics.* 2004; 20:3246–8. [PubMed: 15180930]
22. Edgar R, Domrachev M, Lash AE. Gene Expression Omnibus: NCBI gene expression and hybridization array data repository. *Nucleic Acids Res.* 2002; 30:207–10. [PubMed: 11752295]
23. Hanley JA, McNeil BJ. The meaning and use of the area under a receiver operating characteristic (ROC) curve. *Radiology.* 1982; 143:29–36. [PubMed: 7063747]
24. Gregori S, Tomasoni D, Pacciani V, Scirpoli M, Battaglia M, Magnani CF, et al. Differentiation of type 1 T regulatory cells (Tr1) by tolerogenic DC-10 requires the IL-10-dependent ILT4/HLA-G pathway. *Blood.* 2010; 116:935–44. [PubMed: 20448110]

25. Rutella S, Bonanno G, Procoli A, Mariotti A, de Ritis DG, Curti A, et al. Hepatocyte growth factor favors monocyte differentiation into regulatory interleukin (IL)-10++IL-12low/neg accessory cells with dendritic-cell features. *Blood*. 2006; 108:218–27. [PubMed: 16527888]
26. Krispin A, Bledi Y, Atallah M, Trahtemberg U, Verbovetski I, Nahari E, et al. Apoptotic cell thrombospondin-1 and heparin-binding domain lead to dendritic-cell phagocytic and tolerizing states. *Blood*. 2006; 108:3580–9. [PubMed: 16882710]
27. Pulendran, B., Tang, H., Manicassamy, S. *Nat Immunol*. Vol. 11. Nature Publishing Group; 2010. Programming dendritic cells to induce T(H)2 and tolerogenic responses; p. 647-55.
28. Whiteside TL. Immune modulation of T-cell and NK (natural killer) cell activities by TEXs (tumour-derived exosomes). *Biochem Soc Trans*. 2013; 41:245–51. [PubMed: 23356291]
29. Whiteside TL. Immune suppression in cancer: Effects on immune cells, mechanisms and future therapeutic intervention. *Semin Cancer Biol*. 2006; 16:3–15. [PubMed: 16153857]
30. Vasaturo A, Di Blasio S, Peeters DGa, de Koning CCH, de Vries JM, Figdor CG, et al. Clinical Implications of Co-Inhibitory Molecule Expression in the Tumor Microenvironment for DC Vaccination. A Game of Stop and Go. *Front Immunol*. 2013; 4:417. [PubMed: 24348481]
31. Hargadon KM. Tumor-altered dendritic cell function: implications for anti-tumor immunity. *Front Immunol*. 2013; 4:192. [PubMed: 23874338]
32. Decker P, Kötter I, Klein R, Berner B, Rammensee HG. Monocyte-derived dendritic cells over-express CD86 in patients with systemic lupus erythematosus. *Rheumatology (Oxford)*. 2006; 45:1087–95. [PubMed: 16527880]
33. van den Heuvel MM, Vanhee DD, Postmus PE, Hoefsmit EC, Beelen RH. Functional and phenotypic differences of monocyte-derived dendritic cells from allergic and nonallergic patients. *J Allergy Clin Immunol*. 1998; 101:90–5. [PubMed: 9449506]
34. Cuellar A, Santander SP, Thomas MDC, Guzmán F, Gómez A, López MC, et al. Monocyte-derived dendritic cells from chagasic patients vs healthy donors secrete differential levels of IL-10 and IL-12 when stimulated with a protein fragment of *Trypanosoma cruzi* heat-shock protein-70. *Immunol Cell Biol*. 2008; 86:255–60. [PubMed: 18180802]
35. Kvistborg P, Bechmann CM, Pedersen AW, Toh HC, Claesson MH, Zocca MB. Comparison of monocyte-derived dendritic cells from colorectal cancer patients, non-small-cell-lung-cancer patients and healthy donors. *Vaccine*. 2009; 28:542–7. [PubMed: 19837091]
36. Butterfield LH. Dendritic Cells in Cancer Immunotherapy Clinical Trials: Are We Making Progress? *Front Immunol*. 2013; 4:454. [PubMed: 24379816]
37. Wurfel MM, Park WY, Radella F, Ruzinski J, Sandstrom A, Strout J, et al. Identification of high and low responders to lipopolysaccharide in normal subjects: an unbiased approach to identify modulators of innate immunity. *J Immunol*. 2005; 175:2570–8. [PubMed: 16081831]
38. Peng, JC., Abu Bakar, S., Richardson, MM., Jonsson, JJ., Frazer, IH., Nielsen, LK., et al. *Immunol Cell Biol*. Vol. 84. Nature Publishing Group; 2006. IL10 and IL12B polymorphisms each influence IL-12p70 secretion by dendritic cells in response to LPS; p. 227-32.
39. Beckebaum S, Zhang X, Chen X, Yu Z, Frilling A, Dworacki G, et al. Increased levels of interleukin-10 in serum from patients with hepatocellular carcinoma correlate with profound numerical deficiencies and immature phenotype of circulating dendritic cell subsets. *Clin Cancer Res*. 2004; 10:7260–9. [PubMed: 15534100]
40. Bellone G, Carbone A, Smirne C, Scirelli T, Buffolino A, Novarino A, et al. Cooperative induction of a tolerogenic dendritic cell phenotype by cytokines secreted by pancreatic carcinoma cells. *J Immunol*. 2006; 177:3448–60. [PubMed: 16920987]
41. Fu íková, J., Rožková, D., Ul ová, H., Budinský, V., Sochorová, K., Pokorná, K., et al. *J Transl Med*. Vol. 9. BioMed Central; 2011. Poly I: C-activated dendritic cells that were generated in CellGro for use in cancer immunotherapy trials; p. 223
42. Lurquin C, Lethé B, De Plaen E, Corbière V, Théate I, van Baren N, et al. Contrasting frequencies of antitumor and anti-vaccine T cells in metastases of a melanoma patient vaccinated with a MAGE tumor antigen. *J Exp Med*. 2005; 201
43. Lonchay C, van der Bruggen P, Connerotte T, Hanagiri T, Coulie P, Colau D, et al. Correlation between tumor regression and T cell responses in melanoma patients vaccinated with a MAGE antigen. *Proc Natl Acad Sci U S A*. 2004; 14631–8. [PubMed: 15452345]

44. Van Elssen CHMJ, Oth T, Germeraad WTV, Bos GMJ, Vanderlocht J. Natural Killer Cells: The Secret Weapon in Dendritic Cell Vaccination Strategies. *Clin Cancer Res.* 2014; 20
45. Palucka K, Banchereau J. Cancer immunotherapy via dendritic cells. *Nat Rev Cancer.* 2012; 12:265–77. [PubMed: 22437871]
46. Kamath AT, Sheasby CE, Tough DF. Dendritic cells and NK cells stimulate bystander T cell activation in response to TLR agonists through secretion of IFN-alpha beta and IFN-gamma. *J Immunol.* 2005; 174:767–76. [PubMed: 15634897]
47. Gabrilovich DI, Nagaraj S. Myeloid-derived suppressor cells as regulators of the immune system. *Nat Rev Immunol.* 2009; 9:162–74. [PubMed: 19197294]
48. Chang CH, Qiu J, O'Sullivan D, Buck MD, Noguchi T, Curtis JD, et al. Metabolic Competition in the Tumor Microenvironment Is a Driver of Cancer Progression. *Cell.* 2015; 162:1229–41. [PubMed: 26321679]
49. Zarour HM. Reversing T-cell Dysfunction and Exhaustion in Cancer. *Clin Cancer Res.* 2016; 22
50. Steinman RM, Banchereau J. Taking dendritic cells into medicine. *Nature.* 2007; 449:419–26. [PubMed: 17898760]
51. Bray SM, Vujanovic L, Butterfield LH. Dendritic cell-based vaccines positively impact natural killer and regulatory T cells in hepatocellular carcinoma patients. *Clin Dev Immunol.* 2011; 2011:249281. [PubMed: 21969837]
52. Jansen BJH, Sama IE, Eleveld-Trancikova D, van Hout-Kuijter MA, Jansen JH, Huynen MA, et al. MicroRNA genes preferentially expressed in dendritic cells contain sites for conserved transcription factor binding motifs in their promoters. *BMC Genomics.* 2011; 12:330. [PubMed: 21708028]
53. Aldinucci A, Rizzetto L, Pieri L, Nosi D, Romagnoli P, Biagioli T, et al. Inhibition of immune synapse by altered dendritic cell actin distribution: a new pathway of mesenchymal stem cell immune regulation. *J Immunol.* 2010; 185:5102–10. [PubMed: 20889545]
54. Zhang XL, Peng J, Sun JZ, Liu JJ, Guo CS, Wang ZG, et al. De novo induction of platelet-specific CD4(+)CD25(+) regulatory T cells from CD4(+)CD25(-) cells in patients with idiopathic thrombocytopenic purpura. *Blood.* 2009; 113:2568–77. [PubMed: 19056692]
55. Jiang A, Bloom O, Ono S, Cui W, Unternaehrer J, Jiang S, et al. Disruption of E-cadherin-mediated adhesion induces a functionally distinct pathway of dendritic cell maturation. *Immunity.* 2007; 27:610–24. [PubMed: 17936032]

### Translational relevance

Dendritic cell-based vaccines have been widely tested in preclinical and phase I/II clinical studies, most of which led to unsatisfactory results. Here, we analyzed in depth dendritic cells used in a clinical trial vaccinating prostate carcinoma patients and correlated DC phenotype with clinical and immunological response. Our analysis revealed a gene signature of tolerogenic DC that was minimally expressed in patients showing a strong immunological and clinical response. In parallel, it was observed that a similar predictive value could be obtained using a four-protein index based on CD14 expression on DC membrane, and secretion levels of IL-10, MCP-1 and MDC. These results, if further validated in larger studies, could be used to tailor DC vaccination only to those patients showing low tolerogenic signature in their DC. Furthermore, our study provides a framework that can be used for other cell therapies to identify markers correlating with clinical response.

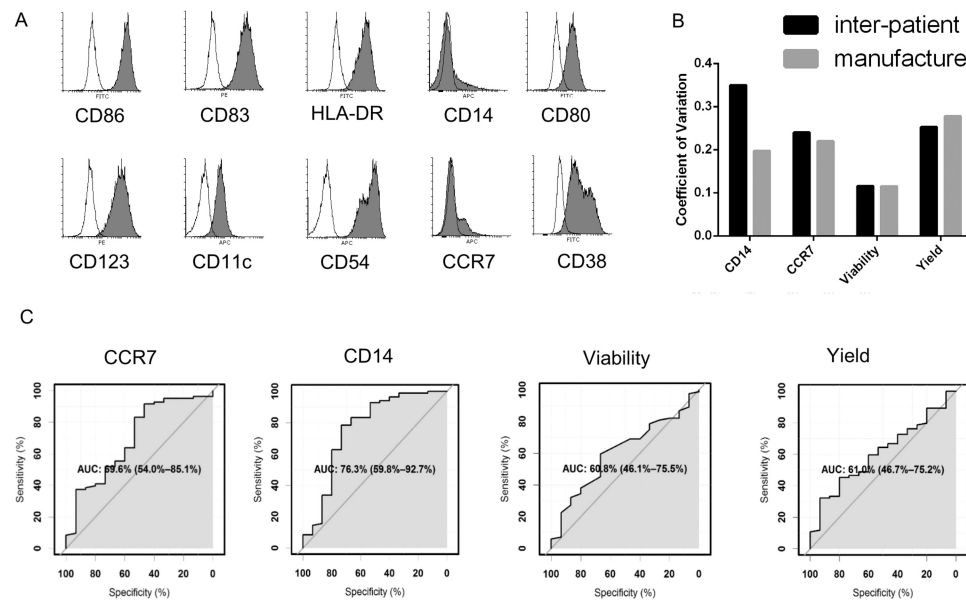


**Figure 1. Flow Cytometry and Culture Data Analysis**

**A)** Flow cytometry analysis of DC. Histograms of the expression of surface markers CD86, CD83, HLA-DR, CD14, CD80, CD123, CD11c, CD54, CCR7, CD38 of a representative DC product; **B)** Coefficients of Variation(CV) of % of CD14+, % CCR7+, % of viable cells and final DC Yields (as a percentage of final number of viable DC compared to total starting number of monocytes) were calculated for manufacturing (light-grey bars) and inter-patient variability (black bars) among all manufactured DC. Manufacturing related CV was calculated as the average CV registered among all the DC generated from each patient, whereas inter-patient CV was calculated on patients averaged values; **C)** ROC curves showing the power of % of CD14+, % CCR7+, % of viable cells, and final DC Yields to discriminate among RespDC and NonRespDC. In a ROC curve plot, the “true positive” diagnosis rate (sensitivity) is plotted against the “false positive” diagnosis rate (1-specificity) for a test with a binary outcome. The AUC summarizes the discrimination of the test, i.e., its ability to classify cases correctly. A perfect test would have an AUC of 100%; a worthless test would have an AUC of 50%. AUC values may be classified as follows: 90%–100%, excellent; 80%–90%, good; 70%–80%, fair; 60%–70%, poor; 50%–60%, fail (23).

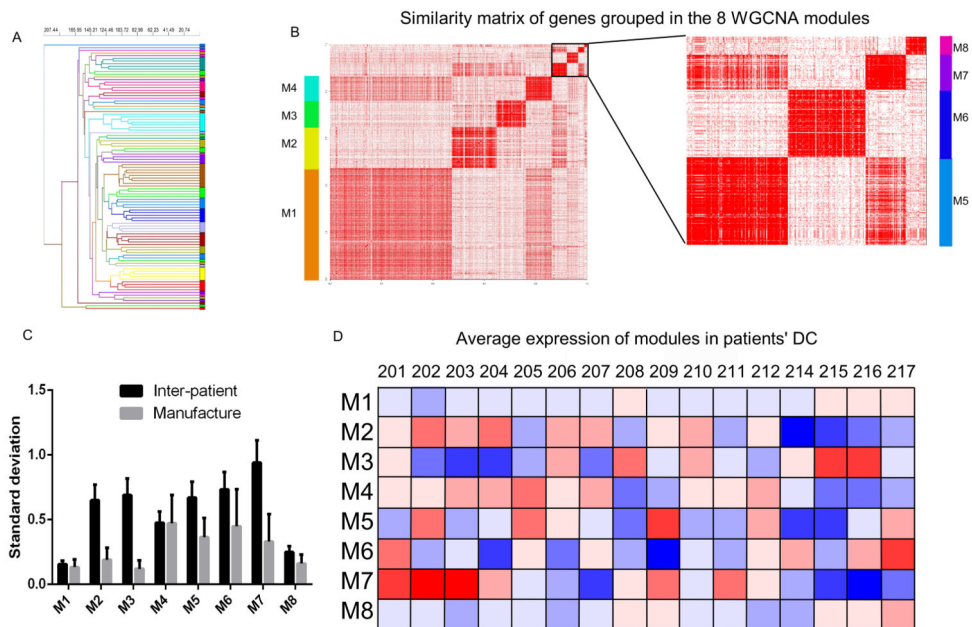


**Figure 2. Gene expression analysis of DC**

DC products (n=99) were analyzed by gene expression profiling using Agilent microarrays.

**A)** Unsupervised hierarchical clustering of the DC based on the whole dataset (35753 genes). Branches are colored according to patient; **B)** Similarity matrix analysis of the 1864 genes belonging to the 8 modules identified by WGCNA. On the right, magnification of the top right corner of the matrix to show less abundant modules. Similarity matrix is on a white-to-red gradient, where white represents a correlation equal to 0, whereas red is 1; **C)** Manufacturing and inter-patient variability of the expression levels of the 8 modules in clinical DC. For each module, the standard deviation of module expression is shown for both inter-patient (black bars) and manufacturing variability (grey bars). Manufacturing variability was calculated as the average standard deviation registered among all the DC generated from each patient, whereas inter-patient variability was calculated on patients averaged values; **D)** Average expression levels of the 8 identified modules in the DC of each patient. The heatmap is shown on a Blue-White-Red Gradient, where blue represents an expression level below the average, white is an average expression level and red represents an expression above the average.



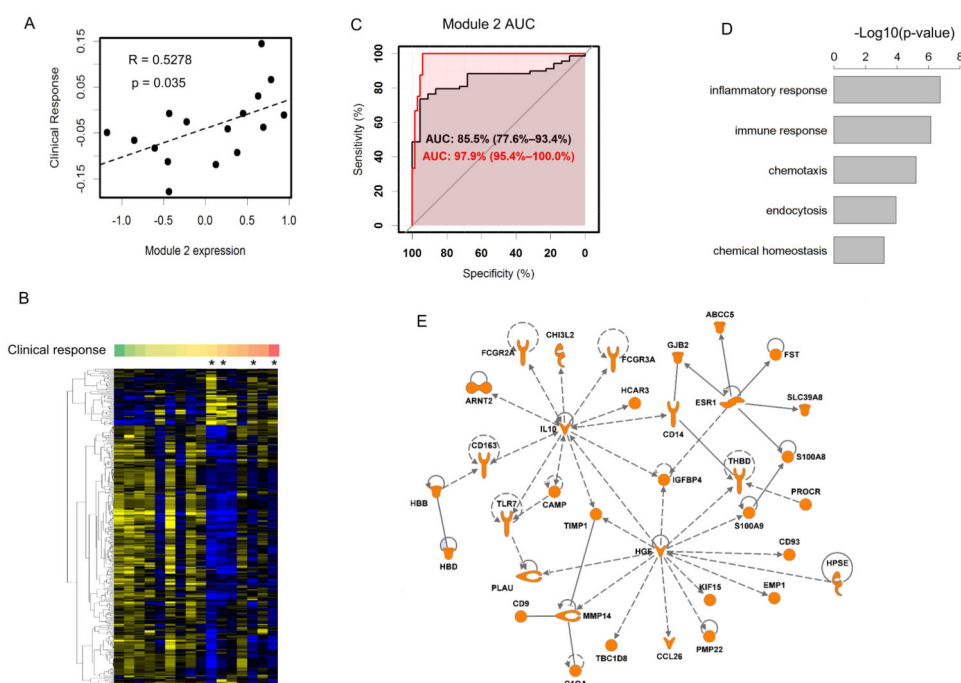


**Figure 3. Module 2 characterization: correlation with response, gene ontology and network analysis**

**A)** Plot showing the correlation of module 2 expression in DC products and the quantitative measure of clinical response at week 48 (measured as the decrease in slope (log PSA) over time); **B)** Heatmap of the patient-averaged expression level of the genes belonging to module 2. Each column represents the average value observed among the DC manufactured from the same patient. Columns are ordered according to the quantitative measure of clinical response at week 48 with non-responders on left shown by the color bar on the top of the heatmap (green: no response, yellow: mild response, red: strong response). \* indicates DC of patients showing strong immunological response (median ELISPOT count >500). Heatmap is coloured on a blue-black-yellow gradient. The top gene cluster of the heatmap shows genes more expressed in Resp-DC whereas the lower cluster shows genes more expressed in NonResp-DC. **C)** ROC curves showing the ability of module 2 expression on DC to discriminate among clinical responders and clinical non-responders in black and strong immunological responders vs non-strong immunological responders in red; **D)** Gene ontology analysis of genes belonging to module 2. P-value of the enrichment of each Biological Process family is shown; **E)** The most relevant network of the genes in module 2 indicated by Ingenuity Pathway Analysis

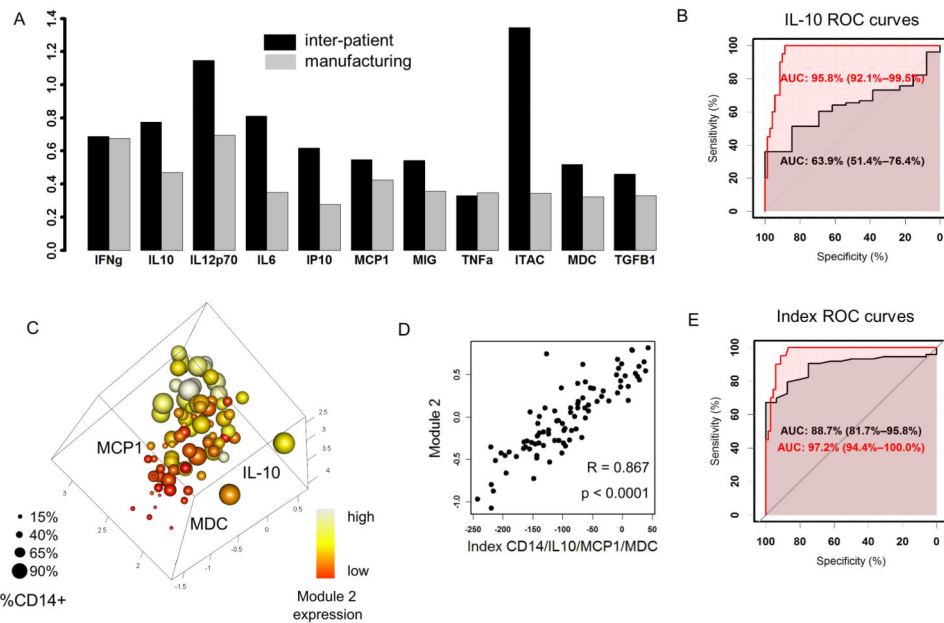


**Figure 4. Cytokine/chemokine secretion profile analysis of DC**

**A)** Coefficients of Variation (CV) of supernatant concentrations of indicated cytokines/chemokines calculated for manufacturing (grey bars) and inter-patient variability (black bars) among 93 manufactured DC products. Manufacturing related CV was calculated as the average CV registered among all the DC generated from each patient, whereas inter-patient CV was calculated on patient-averaged values; **B)** ROC curves showing the ability of IL-10 concentrations measured on DC supernatants to discriminate among clinical and clinical non-responders in black and strong immunological responders vs not-strong immunological responders in red; **C)** Correlation of module 2 expression with CD14, IL-10, MDC and MCP-1. Each dot represents one DC sample. X, y and z coordinates represent concentration levels of IL-10, MDC, and MCP-1, respectively, size of dots is proportional with % of CD14+ cells, color represents module 2 expression level (red-yellow-white gradient, with red being the lowest expression level and white the highest). An interactive 3D plot is available in supplemental figure 3; **D)** Plot showing the correlation of module 2 expression with the CD14+/IL-10/MCP-1/MDC index; **E)** ROC curves showing the ability of CD14+/IL-10/MCP-1/MDC index to discriminate among clinical responders and non-responders in black and strong immunological responders vs not-strong immunological responders in red.

Table 1

## Clinical and immunological patient responses

ID	Gleason score	Baseline PSA concentration	Baseline PSA doubling time (mo)	PSA doubling time at week 48 (mo)	Baseline log PSA slope	Log PSA slope at week 48	Clinical Response at week 24*	Intensity of clinical response at week 24 <sup>a</sup>	Clinical Response at week 48	Intensity of clinical response at week 48 <sup>a</sup>	Immuno-logical response	Intensity of immunological response <sup>b</sup>
201	8	0.91	6.4	43.3	0.109	0.016	Yes	-0.172	Yes	-0.093	No	0
202	7	4.99	12.8	16.1	0.054	0.043	Yes	-0.017	Yes	-0.011	Yes	210
203	7	1.94	6.0	2.7	0.116	0.260	No	0.144		Off Study	Yes	30
204	8	0.96	5.9	3.8	0.118	0.184	No	0.039	No	0.066	No	50
205	9	4.78	2.9	11.4	0.239	0.061	Yes	-0.148	Yes	-0.178	Yes	1180
206	7	0.52	5.1	4.2	0.137	0.167	No	0.036	No	0.03	Yes	100
207	6	3.53	10.5	12.0	0.066	0.058	Yes	-0.002	Yes	-0.008	No	0
208	6	12.00	6.3	8.3	0.110	0.084	Yes	-0.054	Yes	-0.026	No	0
209	6	1.33	7.0	-34.7	0.099	-0.020	Yes	-0.018	Yes	-0.119	No	0
210	4	13.00	12.2	36.5	0.057	0.019	Yes	-0.052	Yes	-0.038	No	0
211	9	1.41	4.1	12.4	0.169	0.056	Yes	-0.087	Yes	-0.113	Yes	710
212	9	5.88	3.7	4.7	0.187	0.146	Yes	-0.002	Yes	-0.041	No	0
214	7	17.30	8.8	23.8	0.079	0.030	Yes	-0.028	Yes	-0.049	Yes	4480
215	7	9.39	5.5	11.5	0.126	0.060	Yes	-0.103	Yes	-0.066	Yes	4370
216	7	1.80	7.5	68.7	0.093	0.010	Yes	-0.013	Yes	-0.083	Yes	230
217	8	0.95	7.9	8.2	0.088	0.080	Yes	-0.028	Yes	-0.008	No	0
218	9	0.48	12.6	/	0.055	/	Yes	-0.025	/	/	Yes	50
220	9	1.00	4.4	/	0.160	/	Yes	-0.07	/	/	Yes	90

\* Absence or presence of a clinical response was defined as having negative difference in the slope log PSA at either 24 or 48 weeks minus the pre-treatment slope log PSA.

<sup>a</sup> Intensity of clinical response was calculated as the difference in slope of PSA trend over time observed at time of analysis compared to pretreatment value (e.g., log PSA slope at week 24 –log PSA slope before treatment)

<sup>b</sup> Intensity of immunological response was calculated as the median # of spots observed through 7d *in vitro* stimulation ELISPOT against wild type 27-35, epitope enhanced 29-37-9V and wild type 29-37 TARP peptides tested at week 12, 18 and 24

/ Not Available

ND: not done

Author Manuscript

Author Manuscript

Author Manuscript

Author Manuscript

**Table 2**  
**Meta-analysis of tolerogenic DC dataset**

Dataset # (Source)	DC Comparison	Publication	p-value of overlap with module 2	Top 20 genes in common with module 2 (only for significantly overlapping)
<b>GSM468775 (NCBI GEO)</b>	IL-10/IL-6 mDCs vs mDCs	(10)	3.56E-06	TGFB1, TIMP1, GLUL, MMP14, ALDH1A1, ABCA1, MMP2, EPAS1, MSR1, CTSC, DOCK4, IPR2, AFB, CD14, SLCO2B1, CCL26, MS4A4A, CYP3A5, PMP22, AGPAT4,
<b>GSE23371 (NCBI GEO)</b>	IL10/dexamethason DC vs LPS DC	(52)	7.34E-06	CD163, CD14, C3AR1, MS4A6A, RNASE1, S100A8, LAIR1, PDK4, FCGR2A, SLCO2B1, C1QA, TMEM37, MLFML2B, GLUL, STAB1, S100A9, CD300LF, GIMAP1, NPL, C5AR1
<b>GSE18921 (NCBI GEO)</b>	IL-10/IL6 DC vs standard DC	(10)	7.52E-06	TGFB1, TIMP1, GLUL, MMP14, ALDH1A1, ABCA1, MMP2, EPAS1, MSR1, CTSC, ITPR2, MAFB, CD14, SLCO2B1, CCL26, MS4A4A, CYP3A5, PMP22, FST, P2RY1
<b>MTAB-286 (EMBL-EBI)</b>	DC grown in presence of MSC vs normal DC	(53)	7.34E-05	CD163, P2RY6, FOLR2, CCR1, SLCO2B1, S100A9, HBB, FCAR, CTS13, CTSC, ALDH1A1, IL10, GATM, TNFRSF6B, S100A12, S100A8, TAGAP, C1QA, NLN, ITPR2
<b>GSE18921 (NCBI GEO)</b>	IL-10 DC vs standard DC	(10)	0.005962	TIMP1, TGFB1, GLUL, MAFB, MMP14, EPAS1, ABCA1, FST, AGPAT4, HIP1, CD14, CTSC, PMP22, SLC39A8, CMKLR1, ITPR2, ALDH1A1, ADAMTS2, FOLR2, P2RY1
<b>GSE7387 (NCBI GEO)</b>	Comparison of gene expression data from induced-regulatory T cell treated- and untreated-DCs from patients with ITP	(54)	>0.05	
<b>GSE9241 (NCBI GEO)</b>	E-cadherin-stimulated DCs vs bacteria activated DCs	(55)	>0.05	
<b>GSE18921 (NCBI GEO)</b>	IL-10/TGFb1 DC vs standard DC	(10)	>0.05	